

The cyclisation of substituted phthalanilic acids in acetic acid solution. A kinetic study of substituted *N*-phenylphthalimide formation

2 PERKIN

Christopher J. Perry* and Zahida Parveen

School of Applied Sciences, The University of Wolverhampton, Wolverhampton, UK WV1 1SB

Received (in Cambridge, UK) 18th October 2000, Accepted 31st January 2001

First published as an Advance Article on the web 23rd February 2001

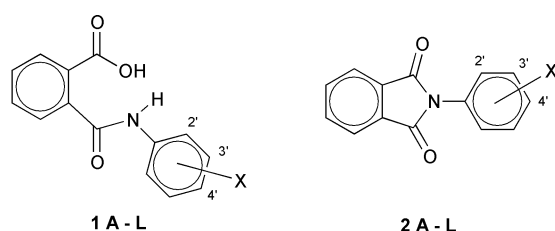
One novel and ten known substituted 3'- and 4'-phthalanilic acids have been prepared. These have been cyclised to two novel and nine known substituted *N*-phenylphthalimides by heating with glacial acetic acid. Both phthalanilic acids and imides have been characterised in detail and spectroscopic data are given. The kinetics of cyclisation for phthalanilic acids has been examined in detail, and it has emerged that a complex mechanism is operating. This initially involves a reversible, solvent assisted intramolecular nucleophilic attack by amide nitrogen on the carboxylic acid carbonyl. Clear evidence is seen for a long-lived intermediate as a precursor to imide formation. The observed kinetics are rationalised using a model of rapid pre-equilibration, followed by the slow breakdown of the intermediate to imide. Observed rate constants for pre-equilibration show a well behaved, linear Hammett plot ($\rho = -1.1$), whereas those for formation of imide do not.

Introduction

There has been a recent resurgence of interest in *N*-phenylphthalimide derivatives and analogues because of their potential in a number of areas such as aminopeptidase inhibition,¹ anticonvulsant activity² and promotion of tumour necrosis factor alpha (TNF alpha) production.³ Substituted phthalamic and phthalanilic acids and their modes of hydrolysis have been the subjects of a number of studies.⁴⁻⁶ However, their cyclisation to the corresponding imides has received less attention. In an earlier paper⁷ it was reported that 2'-aminophthalanilic acid (**1L**) undergoes an anomalous cyclisation to imide **2L** in dilute

aniline analogues to phthalic anhydride and its derivatives, the simple cyclisation procedures reported here demonstrate the potential to prepare a wide range of phthalimides, some of which have previously been prepared by more involved routes.^{17,18} Furthermore, the need for a significant excess of amine which has been suggested in other preparations involving the intermediate formation of phthalanilic and phthalamic acids,^{9,15,19} is removed.

Detailed study of the formation of phthalimides in acetic acid reveals a complex mechanism in which two clearly distinct steps are observable in all examples studied. In all cases investigated there is strong evidence for a relatively long-lived intermediate that decays ultimately to the appropriate phthalimide, at rates that are consistent with the appearance of the product in preparative experiments.



X = A: 4'-COOH, B: 3'-Cl, C: 4'-Cl, D: 4'-OH, E: 3'-OCH₃, F: 4'-OCH₃,
G: 4'-CH₃, H: 3'-NO₂, I: 4'-NO₂, J: -H, K: 4'-SO₃⁻C₃H₅NH⁺, L: 2'-NH₂.

aqueous acid, in contrast to other examples where hydrolysis is the major reaction. The literature contains a few examples of phthalamic acid analogues forming imides in water,⁸ ethanol⁹ and acetic acid,¹⁰ but the number and scope of available studies are limited, as are the published spectroscopic data for phthalanilic acids and phthalimides,¹¹⁻¹⁴ which consist largely of IR and UV data for the imides. Although some work has been undertaken to investigate the possible mechanisms of phthalimide formation in the molten state^{15,16} we have only been able to find one reference to a solution phase study reported in the literature.⁶

In this study we have observed that on heating or refluxing in glacial acetic acid, all examples of substituted phthalanilic acids prepared underwent cyclisation to the corresponding *N*-phenylphthalimide derivatives, in good yields, at varying rates depending upon ring substitution. Since many substituted phthalanilic acids are easily prepared from the addition of

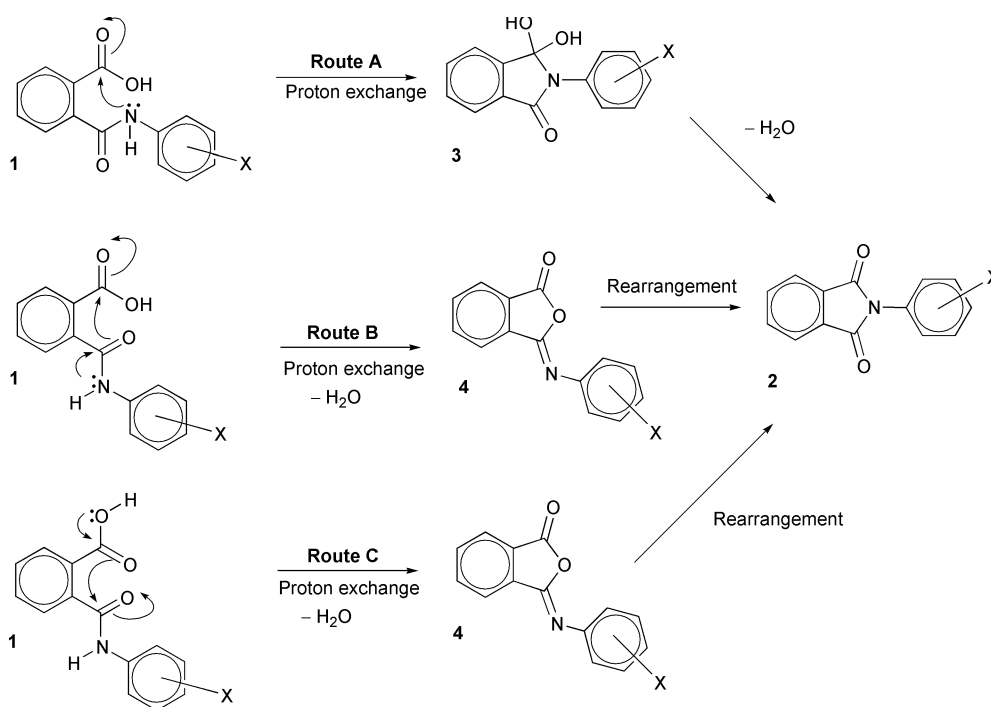
Results and discussion

The substituted phthalanilic acids in this study were prepared by the reaction of substituted anilines with phthalic anhydride in a suitable solvent (usually chloroform). One of the phthalanilic acids (**1K**), and two of the imides (**2A** and **2K**) appear to be new compounds as no physical data could be located in the literature. The general method described proved very effective for obtaining mostly good yields of high purity material without recourse, in the majority of cases, to prolonged reaction times or involved methods and work-up procedures. However, despite the relative ease with which **1L** has been prepared from *o*-phenylenediamine and phthalic anhydride,^{7,20} it did not prove possible to prepare pure 3'- and 4'-aminophthalanilic acids by an analogous method, despite several attempts. Products were obtained, but these appeared to consist of more than one compound and could not be separated by recrystallisation. These mixtures appear to arise from acylation at both amino groups of the diamine in addition to the intended mono-acylation. This side reaction could not be controlled by changes in concentration or addition order, and appeared to be complicated by cyclisation to imide and diimide during recrystallisation attempts.

The cyclisation–dehydration of phthalanilic acid and its analogues in glacial acetic acid solvent is conveniently followed by changes in the UV absorption spectrum. Table 1 summarises

Table 1 Estimates of molar absorptivities ($\epsilon/\text{dm}^3 \text{ mol}^{-1} \text{ cm}^{-1}$) at 275 and 340 nm for the reactants (**1A–1K**) and final products (**2A–2K**) in the cyclisation of phthalanilic acids. Also shown are the ratios for molar absorptivities of product to reactant (ϵ_2/ϵ_1) and the experimentally observed ratios for final absorbance to initial absorbance ($\text{Abs}_x/\text{Abs}_0$). Relevant data for isoimide **4F** are also included

Compound	ϵ_{275}	ϵ_{340}	Compound	ϵ_{275}	ϵ_{340}	275 nm		340 nm	
						ϵ_2/ϵ_1	$\text{Abs}_x/\text{Abs}_0$	ϵ_2/ϵ_1	$\text{Abs}_x/\text{Abs}_0$
1A	14113	1126	2A	11285	236	0.80	0.60	0.21	4.50
1B	5536	567	2B	2255	258	0.41	0.43	0.45	6.2
1C	8529	591	2C	2536	417	0.30	0.49	0.71	3.53
1D	6601	1228	2D	4330	430	0.66	0.84	0.35	1.72
1E	5732	1044	2E	4600	478	0.80	0.92	0.46	7.40
1F	9397	1862	2F	6276	689	0.67	0.81	0.37	2.16
1G	5888	901	2G	5856	595	0.99	0.73	0.66	2.26
1H	13079	2201	2H	6080	487	0.47	—	0.22	—
1I	5496	6320	2I	13858	1373	2.52	1.90	0.22	1.11
1J	4564	831	2J	1605	279	0.35	0.46	0.34	7.00
1K	10821	894	2K	3671	734	0.34	0.25	0.82	6.00
						ϵ_2/ϵ_4		ϵ_2/ϵ_4	
4F	6421	7793	2F	6276	689	0.98	0.78	0.09	0.09



Scheme 1 A summary of the possible routes by which phthalanilic acids (**1**) may cyclise to phthalimides (**2**).

the expected and observed changes in absorbance for the examples studied. In all but the 4'-nitro analogue (**1I**), the absorbance is expected to show an overall decrease in absorbance at 275 nm (*i.e.* $\text{Abs}_x/\text{Abs}_0 < 1$) on passing from reactant to product. The approximate nature of the measured absorbance changes should be appreciated, however, in view of the inherent experimental difficulties of determining initial absorbances in evolving systems. A margin of error of $\pm 20\%$ in the ratios expressed would be realistic. At 275 nm observations are in quite good agreement with predictions, adding confidence to the premise that absorbance measurements at this wavelength are faithfully reflecting the passage of phthalanilic acids to imides. The same is not true, however, for the measurements made at 340 nm. In these cases there are unacceptable variations from the predicted absorbance ratios that are not easily explained, but suggest that strongly absorbing by-products are formed in the early stages of the reaction. Evidence for this lies in the observation that the 'excess absorbance' at 340 nm (see Table 1) is accrued early (in a similar time scale to pre-equilibration), and the subsequent absorbance changes give

similar rate constants to the data amassed at 275 nm. However, in view of the lack of a satisfactory explanation for these observations, no data for 340 nm runs are included and all kinetic measurements are confined to absorbance changes at 275 nm. Yields obtained from preparative reactions, ^1H NMR studies in $\text{CD}_3\text{CO}_2\text{D}$ and thin layer chromatography on reaction mixtures, all indicate that such by-products cannot amount to high proportions of the total reaction products and probably do not exceed 10% of total material in the most extreme cases. The precise nature of these by-products is unclear from this study, but the possibility of solvolysis of the amide function⁴ has not been ruled out.

As other workers have suggested,^{15,16} the cyclisation of amic acids can, in principle, proceed through a number of pathways. These are summarised for the relevant phthalanilic acids in Scheme 1. We present evidence that strongly suggests that Route A in Scheme 1 is the observed pathway in the carboxylic acid media used for this study. This is consistent with published findings^{15,16} for the thermolysis of phthalamic acids, where evidence was found for the amide function (rather than the

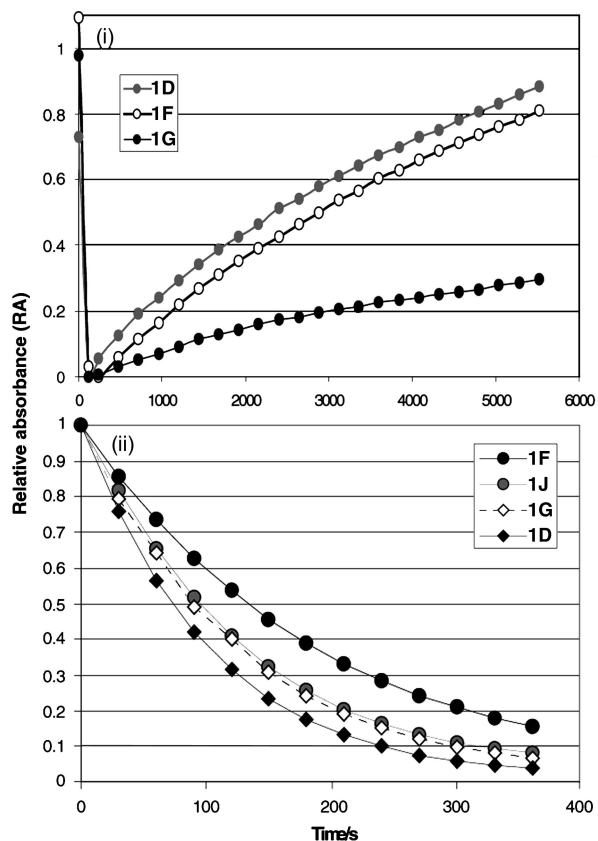


Fig. 1 (i) Relative absorbances at 275 nm observed during the cyclisation of the substituted phthalanilic acids **1D**, **1F** and **1G** at 358 K. (ii) The initial relative absorbance changes observed in (i) (corresponding to the approach to pre-equilibrium), monitored at 317 K. The solvent is glacial acetic acid in all cases. For ease of scaling, presentation and comparison of data the parameter 'relative absorbance' (RA) is used. This is defined for a given kinetic run as $RA = [(Abs_t - Abs_{min})/a]$ where Abs_t = absorbance at time t , Abs_{min} = minimum absorbance observed, and a is a constant (in the above examples between 0.1 and 1.2) whose value is chosen to avoid excessive data overlap. The value of a approximates to $Abs_{init} - Abs_{min}$, where Abs_{init} = initial absorbance.

carboxy function) acting as a nucleophile in the cyclisation reaction, but a distinction between Routes A and B was not resolved.

The most striking feature of the present kinetic study is that in all cases, the absorbance of the reaction mixture rises to a maximum or falls to a minimum (depending on substituent and wavelength) in a relatively short time. This is followed by a much slower rise or decay as the reaction proceeds to effective completion. Fig. 1 shows these changes at 275 nm (317 and 358 K) for a range of compounds in the series studied. The minima observed in these examples are strongly suggestive of the build up of an intermediate,²¹ followed by a slow decay to imide. Similar results were observed at 340 nm and the estimated rates were generally in agreement with those obtained at 275 nm, but for the reasons given earlier, the 340 nm data were felt to be unreliable and have not been included.

Possible intermediates are shown in Scheme 1, as structures **3** and **4**. A sample of the isoimide **4F** was prepared,²² and its

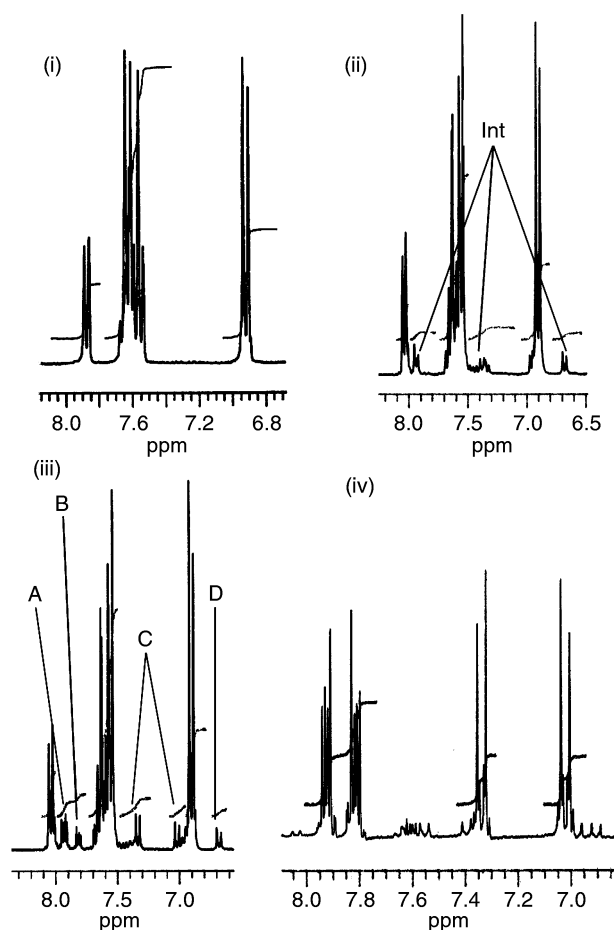
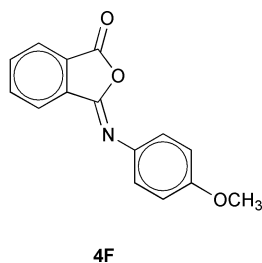


Fig. 2 Changes in the signals from aromatic protons when 4'-methoxyphthalanilic acid (**1F**) reacts in CD_3CO_2D solvent at rt ($\sim 18^\circ C$) to produce imide **2F**. Detail (i) shows the aromatic signals from **2F** in $DMSO-d_6$ for reference. Detail (ii) shows **2F** in CD_3CO_2D after approximately 30 min and reveals new signals attributed to intermediate (labelled Int). After 20 h [detail (iii)] signals due to imide **2F** have also appeared and the signals from intermediate persist in similar proportions to those observed in detail (ii). For explanations of A–D see text. After 37 days [detail (iv)] the signals are largely those of imide **2F**, contaminated with a small amount of starting material (**1F**). Chemicals shifts are relative to an $Me_2Si(CD_2)_2CO_2Na$ standard.

decay to imide **2F** was monitored at 275 and 340 nm. The observed pseudo-first order rate constant for the process at 358 K was determined as $4.0 \times 10^{-3} s^{-1}$; some 24 times faster than the observed rate for the decay of intermediate to imide under similar conditions. It was therefore concluded that structure **4** was not the intermediate for the reaction.

Attempts to isolate the intermediate by quenching reaction mixtures with non-solvents such as diethyl ether or chloroform were unsuccessful and in all cases resulted in the isolation of the starting phthalanilic acid, which became increasingly contaminated with the corresponding imide as reaction times to quenching were increased. These findings suggest either that the concentration of intermediate is low, or that it very rapidly collapses to starting material on quenching. However, in the cases of **1F**, **1D**, and **1I**, 1H NMR experiments were conducted at rt with CD_3CO_2D as the reaction solvent. These examples were chosen for their well-separated aromatic signals and produced convincing evidence for the build up of an intermediate in each case.

For **1F** the intermediate amounted to about 8–16% of the remaining starting material in the reaction system, depending on the chosen interpretation of the intermediate signals. Fig. 2 shows the spectral changes upon which this conclusion is based. After 20 hours [Fig. 2(iii)], signals from starting material (**1F**), imide product (**2F**) and an apparent intermediate are all visible.

The signals labelled A and B are due to the aromatic protons from the phthalimide ring, with signal A also including one of those seen in Fig. 2(ii) at 7.93 ppm due to the intermediate. Signals labelled C correspond to the aromatic protons of the *N*-phenyl ring (4'-methoxy substituted) in the product **2F**. The apparent doublet (D) centred at 6.69 ppm was chosen as the 'marker' for the intermediate as it is clearly separated from other signals. As additional evidence, three signals for $-\text{OCH}_3$ were observed in both the ^1H and ^{13}C NMR spectra throughout most of the reaction for **1F**.

No substantiated assignments have been made for the intermediate signals, but it is conceivable that signal D is due to the two aromatic hydrogens β - to the N atom in structure **3**, and that the other doublet expected from the *N*-(4'-methoxyphenyl) ring is partially concealed by the signals at 6.9 ppm. In this case the 'equilibrium' proportion of intermediate is $\sim 8\%$ of remaining **1F**. What is clear, however, is that the signals for the intermediate are not due to isoimide **4F** as all aromatic protons in this molecule have chemical shifts of ≥ 7.0 ppm as determined in $(\text{CD}_3)_2\text{SO}$ solvent. It is unlikely that chemical shift differences due to solvent changes account for such large discrepancies and the absence of **4F** in the spectrum is the preferred interpretation, being consistent with kinetic evidence. Also, the possibility that these signals arise from a side reaction, as mentioned earlier, was rejected on the grounds that signal D is relatively constant in area (as a proportion of remaining **1F**) for the earlier part of the reaction time but becomes invisible by 37 days.

A similar ^1H NMR study of the changes involved in **1D** \rightarrow **2D** supports the earlier conclusions and provides very clear evidence of the existence of an intermediate. Fig. 3 shows the changes in the signals from the aromatic protons. Most striking is the early appearance of signals (labelled Int) which can be confidently attributed to the *N*-(4'-hydroxyphenyl) ring. Again, the chemical shift of the signal at 6.9 ppm suggests a deprotonated nitrogen in the predominant intermediate structure, and the tripartite nature of the reaction mixture is made very clear in the signals observed between 7.5 and 6.8 ppm. In this case, the 'equilibrium' proportion of intermediate is approximately 35%, calculated from the signals at 7.35 and 7.45 ppm. Again, at near completion (achieved by heating the NMR sample at 90°C for 12 h), only signals from **2D** and traces of impurities remain. In Fig. 3, it is possible to tentatively assign signals to account for structure **3**. 'Doublets' (2H per doublet) at 6.9 and 7.35 ppm account for the four protons of the *N*-(4'-hydroxyphenyl) ring. The signals from the other ring can be seen as the smaller 'doublet' centred at 8.02 ppm (1H), a multiplet in the range 7.91–7.96 ppm (2H) and the remaining 'doublet' (1H) is presumably concealed in the range 7.4–7.7 ppm. Again in the case of **1I**, after 1.5 h at 328 K a very distinct 'doublet' appears at 6.65 ppm that can be attributed to intermediate and suggests an 'equilibrium' constant of ~ 0.65 . The peaks are clearly visible before any signals from imide can be detected.

The evidence discussed above points to Route A in Scheme 1 as the most probable path for the reaction. Interpretation of the kinetic data obtained can be made in terms of a rapid pre-equilibrium between phthalanilic acid and an intermediate, followed by a slow decay to imide, according to Scheme 2.

Because the observed time scale of the prior equilibration (see Table 2) is much shorter than that of the decay of intermediate (*i.e.* $k_1 + k_{-1} \gg k_2$ in Scheme 2), it has proved helpful to approximate by regarding the prior equilibration and the appearance of imide as separate pseudo-first order processes. At 317 K, $-\text{d}[\mathbf{1}]/\text{d}t$ (as monitored by the change in absorbance at 275 nm) is sufficiently slow to allow the approach to equilibrium to be monitored. Using conventional treatments, a value for the empirically derived rate constant for approach to equilibrium (k_e) can be determined for each example.^{23a} Data were analysed using eqn. (1) and the validity of the treatment

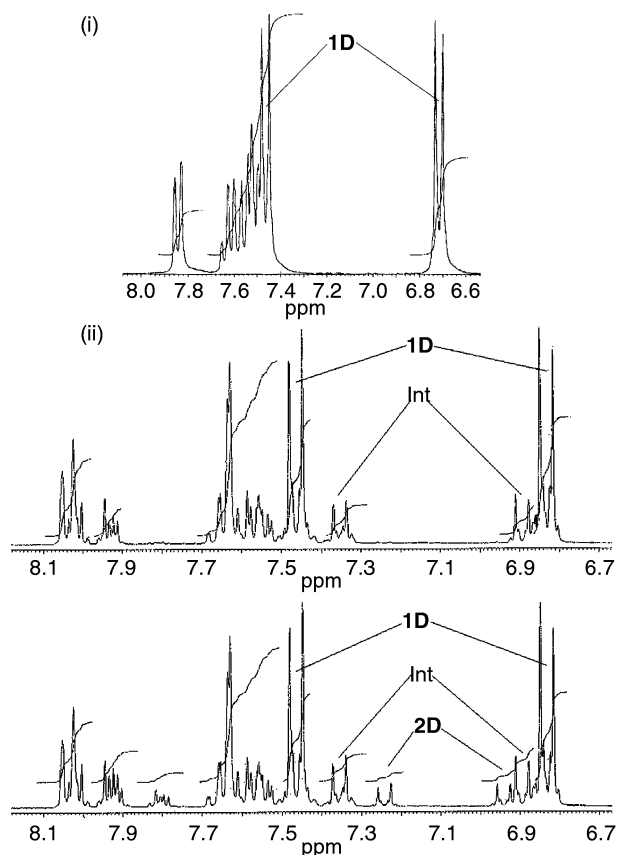


Fig. 3 Changes in the ^1H NMR spectrum of **1D** in $\text{CD}_3\text{CO}_2\text{D}$ solvent at rt (approx. 293 K). (i) A reference spectrum for **1D** in $\text{DMSO}-d_6$. Peaks labelled **1D** are the aromatic protons of the *N*-(4'-hydroxyphenyl) ring. (ii) The upper extract shows the appearance (after 30 min) of new peaks (labelled Int) that are attributed to the *N*-(4'-hydroxyphenyl) ring of an intermediate. The lower extract shows peaks due to imide **2D** in addition to **1D** and intermediate, observed after 24 h. Chemical shifts are relative to an $\text{Me}_2\text{Si}(\text{CD}_2)_2\text{CO}_2\text{Na}$ standard.

$$\ln \left\{ \frac{[\mathbf{1}]_t - [\mathbf{1}]_e}{[\mathbf{1}]_0 - [\mathbf{1}]_e} \right\} = -k_e t \quad (1)$$

was supported by the quality of the fit of experimental results to the function. Correlation coefficients were ≥ 0.998 for all of the data presented and the observed values for k_e are given in Table 2.

The possibilities for partitioning between $3\text{H}^+\text{A}^-$, $3'\text{H}^+\text{A}^-$ and **3** complicate the nature of the pre-equilibrium and the subsequent interpretation of k_e . From ^1H NMR evidence, one of the species accounts for practically all of the intermediate and chemical shifts indicate that this is more likely to be **3** than the two ionic alternatives. This implies that the proton transfer processes in the partitioning of $3\text{H}^+\text{A}^-$ are very fast. Assuming this to be the case, the prior equilibrium becomes $\mathbf{1} + \text{HA} \rightleftharpoons \mathbf{3} + \text{HA}$. The path from **3** to **1** is presumed to be *via* a rapid equilibrium (K' , Scheme 2) between **3** and 3H^+ followed by the rate determining base catalysed ring opening of 3H^+ involving A^- . Provided **HA** is in large excess compared to **1** and **3** it is possible to write eqn. (2). The parameter k_{rev} in eqn. (2) is the apparent rate constant for the back reaction, and

$$\frac{-\text{d}[\mathbf{1}]}{\text{d}t} = k_1[\mathbf{1}][\text{HA}] - k_{\text{rev}}[\mathbf{3}][\text{HA}] \quad (2)$$

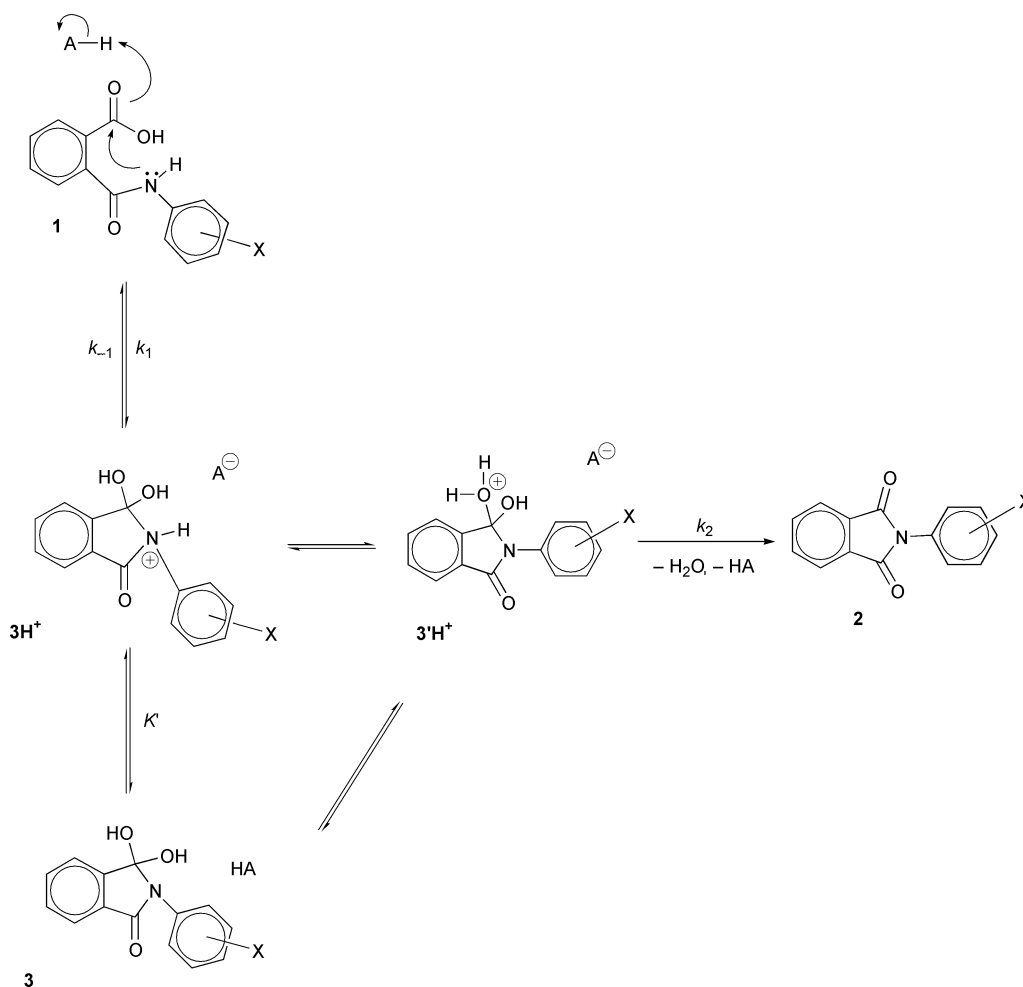
is defined as $k_{\text{rev}} = k_{-1}K'$. Integration of eqn. (2) gives a form of eqn. (1) where k_e is defined by eqn. (3).

$$k_e = (k_1 + k_{\text{rev}})[\text{HA}] \quad (3)$$

Table 2 Observed pseudo-first order rate constants for the initial approach to equilibrium at 317 K ($1X \rightleftharpoons 3X$; k_e) and imide formation at 358 K ($3X \rightarrow 2X$; k_{im}) according to Scheme 2

Compound	X-	$k_e/10^{-4} \text{ s}^{-1}$ (317 K)	$k_{im}/10^{-4} \text{ s}^{-1}$ (358 K)	k_e/k_{im}^a (358 K)	% Yield ^b (calc.)	% Yield ^c (found)
1F	4'-OCH ₃	52.5	1.65	500	77.4	78
1D	4'-OH	124.0	1.90	1040	81.9	80
1G	4'-CH ₃	85.0	2.40	570	88.5	73
1J	H	72.5	1.50	770	74.1	75
1E	3'-OCH ₃	54.6	0.5	1750	36.2	30
1C	4'-Cl	42.3	1.50	450	74.1	61
1B	3'-Cl	32.0	4.50	110	98.3	58
1H	3'-NO ₂	10.8	— ^d	—	— ^d	0 ^e
1A	4'-COOH	9.5	— ^d	—	— ^d	0 ^e
1I	4'-NO ₂	3.3	0.058	910	5.1	0 ^e
1K	4'-SO ₃ ⁻	15.0	2.80	90	92.0	63 ^f

^a Estimated from k_e at 317 K using a doubling in rate for each increase of 10 K. ^b Calculated from k_{im} for a 2.5 h reaction time. ^c From gravimetric determination of imide precipitated from reaction mixture to rt after 2.5 h at 358 K (see Experimental section). ^d Absorbance changes after pre-equilibration are too small for accurate determination of k_{im} . ^e Product isolated was **1X** contaminated with varying proportions of **2X**. ^f 1.5 h reflux (see Experimental section).



Scheme 2 Proposed mechanism for the formation of phthalimides in protic solvents (represented as HA).

Eqn. (3) requires that k_e is dependent upon the concentration of general acid.^{24a,25} Dilution of the carboxylic acid with absolute ethanol produced an observed rate constant (k_e) that was sensibly proportional to the carboxylic acid concentration in the solution. Fig. 4 shows this effect for **1F** and **1J** at 333 K for concentrations up to 10 M acetic acid. Absolute ethanol was chosen as the diluent for the carboxylic acid to avoid hydrolysis and other side reactions, and also because the rate of cyclisation of phthalanilic acids is demonstrably much slower in this solvent. For **1F** the apparent k_e in absolute ethanol was about 200 times smaller at 333 K than that in acetic acid, and the compound could be recrystallised from this solvent without signifi-

cant imide formation. However, some evidence was obtained to suggest that the cyclisation rate of **1F** in ethanol is significantly accelerated by the addition of modest amounts (1–5%) of water. This observation was made as early as 1908.⁹

Also studied were the effects on k_e of varying the composition of the carboxylic acid solvent at 317 K, using **1F** and **1J** as subjects. The observed values for k_e were close to those given in Table 2 ($\pm 10\%$) in pure acetic acid solvent as well as chloroacetic–acetic acid mixtures in the range 10 to 50% (w/v). In TFA, an approximately four-fold increase was observed for **1J**. This observed constancy for the rate over a range of acids of different pK_a values is again consistent with the idea of a

Table 3 Estimates of various constants associated with Scheme 1

Compound	Conditions	K_e ([3]/[1])	$k_e/10^{-2} \text{ s}^{-1}$	$k_1/\text{dm}^3 \text{ 10}^{-4} \text{ s}^{-1} \text{ mol}^{-1}$	$k_{\text{rev}}/\text{dm}^3 \text{ 10}^{-4} \text{ s}^{-1} \text{ mol}^{-1}$	$K_{\text{im}}/10^{-5} \text{ s}^{-1}$	$(k_1 + k_{\text{rev}})/\text{dm}^3 \text{ 10}^{-4} \text{ s}^{-1} \text{ mol}^{-1}$
1D	CD ₃ CO ₂ D, 293 K	0.32 ± 0.02 ^d	—	—	—	—	—
1D	CH ₃ CO ₂ H, 317 K	—	1.24 ^c	1.70 ^a	5.39 ^a	—	7.1 ^a
1F	CD ₃ CO ₂ D, 293 K	0.09 ± 0.02 ^d	—	—	—	~0.1 ^{c,d}	—
1F	CH ₃ CO ₂ H, 317 K	—	0.53 ^c	0.25 ^a	2.76 ^a	—	3 ^a
1F	CH ₃ CO ₂ H, 333 K	—	2.76 ^c	1.3 ^a	14.5 ^a	—	15.8 ^a , 12 ^b
1F	CD ₃ CO ₂ D, 333 K	—	2.98 ^c	1.4 ^a	15.6 ^a	—	17 ^a
1F	CH ₃ CO ₂ H, 358 K	—	—	—	—	16.5 ^c	—
1F	CD ₃ CO ₂ D, 358 K	—	—	—	—	9.2 ^c	—
1I	CD ₃ CO ₂ D, 328 K	0.65 ± 0.05 ^d	—	—	—	—	—
1I	CD ₃ CO ₂ H, 328 K	—	~0.07 ^e	~0.16 ^a	~0.24 ^a	—	~0.4 ^a
1J	CH ₃ CO ₂ H, 333 K	—	1.81 ^c	—	—	—	8.5 ^b
1J	CD ₃ CO ₂ D, 333 K	—	1.96 ^c	—	—	—	—

^a Calculated from k_e and K_e given in this table on the assumption that for K_e there is relatively small temperature dependence and the observation that solvent kinetic isotope effects are relatively small for k_e . ^b Calculated from the slopes in Fig. 4. ^c Directly observed experimentally. ^d Determined from ¹H NMR data. ^e Estimated from value at 317 K.

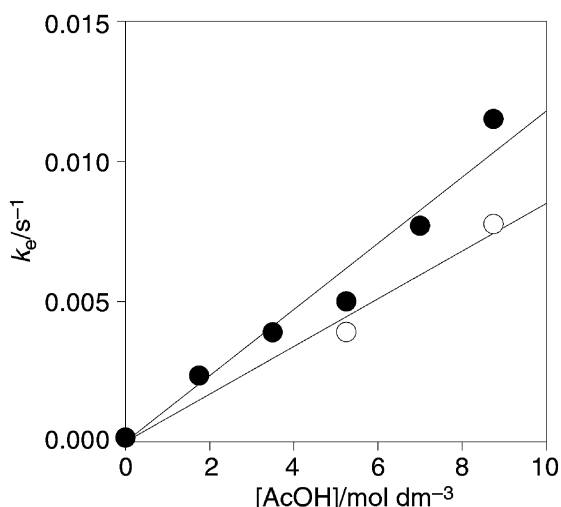


Fig. 4 Variation in observed k_e for **1F** (solid black circles) and **1J** (open circles) at 333 K in acetic acid–ethanol mixtures.

concerted proton transfer with a transition state close in nature to the reactants.^{24a} Solvent deuterium isotope effects were determined for **1F** from kinetic runs in CD₃CO₂D, and k_e was shown to demonstrate a small effect ($k_H/k_D = 0.92$). This small effect seems in keeping with the results above in that the lability of the A–H (or A–D) bond in the carboxylic acid solvent is not a significant rate-determining factor in the approach to equilibrium, and the other proton exchange reactions are very fast.

Eqn. (2) does not allow the resolution of k_1 and k_{rev} without an independent estimate of equilibrium constant. This constant (K_e) was evaluated by NMR in CD₃CO₂D solution for **1F** and **1D**. The values at rt were 0.09 and 0.54 respectively. From these and other values, a number of estimates were made for parameters in Scheme 2, and these are summarised in Table 3.

In view of the absence of evidence for an isoimide intermediate, it seems inevitable that k_e will be influenced by the nucleophilicity of the amide nitrogen of **1X**, as suggested in Scheme 2. More specifically if k_1 and k_{rev} are rate determining, it seems reasonable that substituent effects which increase k_1 will also increase k_{rev} by virtue of an enhanced basicity in the amide nitrogen of **3X**. Fig. 5(i) shows a Hammett plot for the observed values of k_e , which indicates a convincing correlation with σ . Clearly, **1F** and **1K** do not correlate well, and the reasons for this, in the case of **1F**, are not clear since in most other respects the system seems to adhere to the proposed model.

In the **1K** case, however, the poor correlation is more likely to be due to the lack of an appropriate value for σ . It would appear that the 4'-SO₃⁻ substituent is not fully ionised in glacial

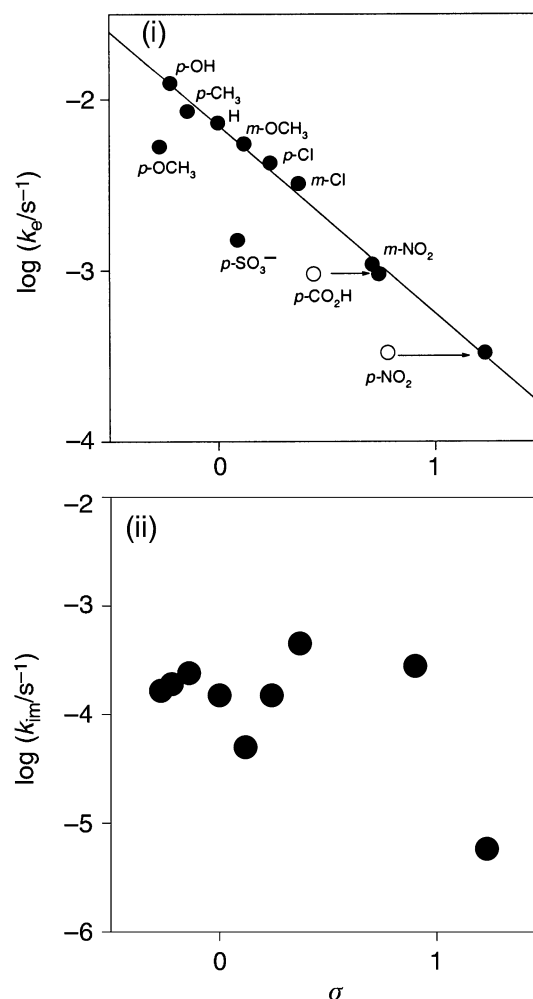
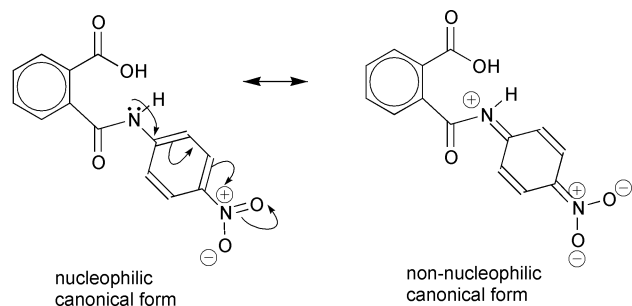


Fig. 5 (i) Plot of $\log(k_e/\text{s}^{-1})$ at 317 K versus σ for the series **1A–1K**. Open circles show cases where σ has been superseded by σ^- in order to achieve correlation. (ii) A similar plot for values of k_{im} , demonstrating a lack of correlation. Data are from Table 2.

acetic acid and is therefore not delivering the expected level of nucleophilic enhancement to the amide nitrogen. Indeed the observed rate is intermediate between that expected for 4'-SO₃R ($\sigma = 0.9$; $\sigma^- = 1.06$) and 4'-SO₃⁻ ($\sigma = 0.09$).^{24b} The simplest explanation for this is that in a solvent with a comparatively low relative permittivity such as acetic acid, there is a significant amount of ion pairing between Ar–SO₃⁻ and the pyridinium ion. The observed rate reflects this increased

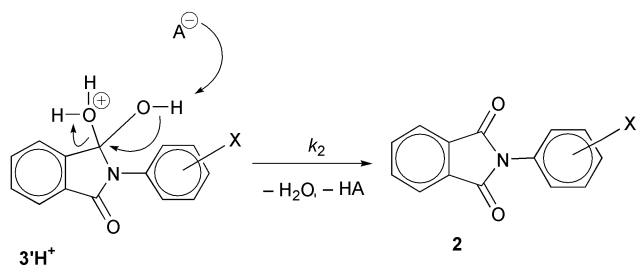
covalent character by showing an apparent substituent constant of ~ 0.63 .

It can be seen from Fig. 5(i) that in the cases of **1A** and **1I**, the correlation for k_e is greatly improved if σ^- is used for the substituent constant in place of σ . If **1F** and **1K** are excluded from the correlation for the reasons discussed, then $\rho = -1.13$ and the correlation coefficient is 0.993. This observation is again consistent with the notion that k_e is influenced by the nucleophilicity of the amide nitrogen. With the 4'-CO₂H and 4'-NO₂ substituents in these examples, through resonance diminishes this nucleophilicity by an amount that is greater than that predicted from σ alone. This can be rationalised as in the following diagram using **1I** as an example.²⁶



At the higher temperature chosen (358 K), it is possible to ignore the very early data and after 'equilibrium' between **1X** and intermediate has been reached, follow the appearance of the imide product. The observed rate constant under these conditions is proportional to k_2 .^{23b} We have referred to this constant as k_{im} to signify its connection with the appearance of imide, and its value for each substituent is given in Table 2. Values determined for k_{im} allow the calculation of a maximum theoretical yield from each preparation conducted in acetic acid using a 2.5 h reaction time at 358 K. The imide products are, in many cases, extremely insoluble in glacial acetic acid as can be seen from the comparison between the calculated and observed yields, given in Table 2.

Fig. 5(ii) shows that k_{im} , unlike k_e does not correlate well with σ . This is consistent with Scheme 3 in that the proposed rate-



Scheme 3 Proposed mechanism for the slow deprotonation of the intermediate in the formation of imide.

determining step does not involve the formation or cleavage of a bond to the nitrogen atom. As a consequence, the ring substituent would be expected to exert only a small influence leading to a poor correlation.

Solvent deuterium isotope effects are more pronounced for k_{im} ($k_H/k_D = 1.79$ for **1F**) than for k_e ($k_H/k_D = 0.92$ for **1J**, 0.93 for **1F**). Assuming rapid and near complete deuterium exchange, this would seem to indicate that breakdown of **3H⁺A⁻** involves the slow cleavage of an O-H (or O-D) bond. A plausible mechanism for this is indicated in Scheme 3. The observation that 'pre-equilibration' occurs, indicates that **3H⁺A⁻** readily undergoes a rapid proton exchange to give **3H⁺A⁻** or loss of proton to **A⁻** to give **3**, but only slowly deprotonates through the route suggested in Scheme 3 to furnish the imide product. One implication of this is that the

spontaneous loss of water from **3H⁺A⁻** to give a carbocation (in resonance with an oxonium or iminium ion) is not the preferred route to product, despite the relative stability of such species. One can therefore suggest that a concerted mechanism such as the one in Scheme 3 is the preferred mode of collapse for **3H⁺A⁻** in view of the low relative permittivity of glacial acetic acid. It is also reasonable that the long lifetime of **3** during the reaction can be partly attributed to the stability gained from hydrogen bonding to acetic acid solvent.

Experimental

Materials

Materials were used as received from the commercial supplier unless stated otherwise in the following methods. Glacial acetic acid as a reaction solvent for kinetic work was prepared from general purpose reagent by distillation through a 30 cm Vigreux column. Deuterated acetic acid (CD₃CO₂D) was obtained from CEA-France (Lot 173-1073) and the glass ampoules were opened immediately prior to use.

Substituted phthalanilic acids (**1A**–**1K**)

Compounds **1A**–**1K** were prepared by a modification of a published method.²⁷ The following general procedure was used unless otherwise specified.

Phthalic anhydride (0.05 mol) and the appropriately substituted aniline (0.05 mol, recrystallised where necessary) were each dissolved in separate portions of chloroform (100 cm³) in 250 cm³ conical flasks. If heating was necessary to dissolve the reactants, the solutions were normally cooled to rt before proceeding. The amine was then added in several portions to the anhydride with thorough mixing between additions. After a moderately exothermic reaction, the mixture was allowed to stand for 30–60 min. Crude products were filtered under vacuum and dried at 80 °C. Purification was by recrystallisation from methanol unless otherwise stated. Molar mass (M_r) values were determined by titration of the purified compound (0.2–0.5 g) in ethanol or aqueous ethanol with 0.1 M NaOH and a phenolphthalein indicator. Potassium hydrogen phthalate was used as the standard. Estimates of M_r by this method are expected to have an accuracy of within $\pm 1\%$. These limits were observed for all cases except the dicarboxylic acid **1A**, where the error was +2.1%. This error may be attributable to a premature end-point if the phenolphthalein indicator is changing colour marginally before the pH at which the dicarboxylic acid ceases to buffer.

NMR spectra were recorded using a JEOL JNM-EX270 FT NMR SYSTEM. All IR spectra were recorded as Nujol mulls. Mass spectrometry data (EI) were obtained only on imides because of decomposition of the phthalanilic acids at, or just above, their melting points. Where published data for the imides is available,¹³ the fragmentation is in good agreement.

2-[(4-Carboxyphenyl)aminocarbonyl]benzoic acid (1A). A solution of phthalic anhydride and a solution/suspension of 4-aminobenzoic acid, prepared as described above, were both raised to bp. After mixing, the flask was stoppered and allowed to stand at rt for 50 h. White solid (95%); mp 281 °C (lit.,²⁷ 280 °C); δ_H (270 MHz; (CD₃)₂SO; Me₄Si) 7.57–7.71 (m, 3H, aryl protons), 7.84 (d, 2H, aryl protons), 7.92–7.98 (m, 3H, aryl protons), 10.69 (s, 1H, CO₂H), 12.96 (br s, 2H, NH, CO₂H); δ_C (68 MHz; (CD₃)₂SO; Me₄Si) 118.36, 124.77, 127.36, 129.19, 129.32, 129.91, 131.41, 138.12, 143.05, 166.33, 166.63, 167.21; ν_{max} /cm⁻¹ 3295 (NH), 1715 (C=O acid), 1690 (C=O acid), 1654 (C=O amide). M_r Found: 291.3. C₁₅H₁₁NO₅ requires 285.26.

2-[(3-Chlorophenyl)aminocarbonyl]benzoic acid (1B). White solid (83%); mp 173–175 °C (lit.,^{4,28} 184, 170–171.5 °C); δ_H (270 MHz; (CD₃)₂SO; Me₄Si) 7.11–7.17 (m, 1H, aryl proton), 7.36

(t, 1H, aryl proton), 7.54–7.70 (m, 4H, aryl protons), 7.89–7.94 (m, 2H, aryl protons), 10.52 (s, 1H, CO₂H), 13.09 (br s, 1H, NH); δ_{C} (68 MHz; (CD₃)₂SO; Me₄Si) 117.40, 118.46, 122.50, 127.21, 129.03, 129.07, 129.26, 129.79, 131.28, 132.46, 137.95, 140.35, 166.51, 166.95; ν_{max} /cm⁻¹ 3310 (NH), 1718 (C=O acid), 1660 (C=O amide). *M_r* Found: 275.69. C₁₄H₁₀NO₃Cl requires 275.9.

2-[(4-Chlorophenyl)aminocarbonyl]benzoic acid (1C). White solid (89%); mp 183–184 °C, (decomposes) (lit.,⁴ 184–185 °C); δ_{H} (270 MHz; (CD₃)₂SO; Me₄Si) 7.40 (d, 2H, aryl protons), 7.55–7.69 (m, 3H, aryl protons), 7.74 (d, 2H, aryl protons), 7.91 (d, 1H, aryl proton), 10.49 (s, 1H, CO₂H), 13.10 (br s, 1H, NH); δ_{C} (68 MHz; (CD₃)₂SO; Me₄Si) 121.06, 126.96, 127.83, 128.61, 129.56, 129.65, 129.93, 131.83, 138.57, 138.72, 167.43, 167.58; ν_{max} /cm⁻¹ 3320 (NH), 1725 (C=O acid), 1640 (C=O amide). *M_r* Found: 274.8. C₁₄H₁₀NO₃Cl requires 275.69.

2-[(4-Hydroxyphenyl)aminocarbonyl]benzoic acid (1D). 4-Aminophenol was recrystallised (with decolourising charcoal) from aqueous ethanol before use and suspended in chloroform (100 cm³) by vigorous magnetic stirring. Pyridine (10 cm³) was added followed by the phthalic anhydride solution. Stirring was continued for 1 h. The product was filtered under vacuum and dried at 80 °C. Off-white solid (82%). Material was purified for analysis by dissolving in saturated KHCO₃, filtering to remove insoluble solids and neutralisation with 6 M HCl. The precipitate was further purified by recrystallisation from ethyl acetate–methanol (85 : 15 approx.). White solid; mp 289–290 °C (lit.,²⁷ 289 °C); δ_{H} (270 MHz; (CD₃)₂SO; Me₄Si) 6.72 (d, 2H, aryl protons), 7.44–7.66 (m, 5H, aryl protons), 7.84 (d, 1H, aryl proton), 9.20 (br s, 1H, OH), 10.0–15.00 approx. (1H, NH), 10.07 (s, 1H, CO₂H); δ_{C} (68 MHz; (CD₃)₂SO; Me₄Si) 114.49, 120.79, 127.24, 128.64, 128.86, 129.69, 130.69, 130.93, 138.37, 152.70, 165.91, 166.88; ν_{max} /cm⁻¹ 3287 (NH), 1714 (C=O acid), 1653 (C=O amide). *M_r* Found 257.2. C₁₄H₁₁NO₄ requires 257.25.

2-[(3-Methoxyphenyl)aminocarbonyl]benzoic acid (1E). White solid (94%); mp 160–161.5 °C (lit.,^{4,9} 171, 159–161 °C); δ_{H} (270 MHz; (CD₃)₂SO; Me₄Si) 3.74 (s, 3H, OCH₃), 6.65–6.68 (m, 1H, aryl proton), 7.19–7.29 (m, 2H, aryl protons), 7.43 (s, 1H, aryl proton), 7.53–7.67 (m, 3H, aryl protons), 7.89 (d, 1H, aryl proton), 10.33 (s, 1H, CO₂H), 13.03 (br s, 1H, NH); δ_{C} (68 MHz; (CD₃)₂SO; Me₄Si) 54.96, 105.06, 108.36, 111.50, 127.30, 128.94 (2C[?]), 129.06, 129.49, 131.20, 138.36, 140.20, 158.84, 166.74, 166.78 (14 signals observed); ν_{max} /cm⁻¹ 3335 (NH), 1725 (C=O acid), 1640 (C=O amide). *M_r* Found 271.0. C₁₅H₁₃NO₄ requires 271.27.

2-[(4-Methoxyphenyl)aminocarbonyl]benzoic acid (1F). The 4-methoxyaniline was recrystallised (with decolourising charcoal) before use. White solid (94%); mp 156–158 °C (lit.,^{4,27} 156–157, 138 °C); δ_{H} (270 MHz; (CD₃)₂SO; Me₄Si) 1.0–6.5 approx. (1H, NH), 3.75 (s, 3H, OCH₃), 6.92 (d, 2H, aryl protons), 7.55–7.67 (m, 5H, aryl protons), 7.87 (d, 1H, aryl proton), 10.32 (s, 1H, CO₂H); δ_{C} (68 MHz; (CD₃)₂SO; Me₄Si) 55.22, 113.46, 120.78, 127.39, 128.88, 129.10, 129.74, 131.19, 132.35, 138.51, 154.81, 166.36, 167.02; ν_{max} /cm⁻¹ 3285 (NH), 1708, 1694 (C=O acid), 1659 (C=O amide). *M_r* Found 272.6. C₁₅H₁₃NO₄ requires 271.27.

2-[(4-Methylphenyl)aminocarbonyl]benzoic acid (1G). White solid (86%); mp 153–154 °C (sinters), 193–195 °C (re-melts) (lit.,^{4,27} 160–161, 155 °C); δ_{H} (270 MHz; (CD₃)₂SO; Me₄Si) 2.26 (s, 3H, CH₃), 7.13 (d, 2H, aryl protons), 7.50–7.67 (m, 5H, aryl protons), 7.87 (d, 1H, aryl proton), 10.25 (s, 1H, CO₂H) 11.0–15.0 approx. (1H, NH); δ_{C} (68 MHz; (CD₃)₂SO; Me₄Si) 20.68, 119.14, 127.31, 128.50, 128.83, 129.02, 129.56, 131.14, 131.73, 136.56, 138.41, 166.48, 166.86; ν_{max} /cm⁻¹ 3315 (NH), 1725

(C=O acid), 1635 (C=O amide). *M_r* Found: 254.1. C₁₅H₁₃NO₃ requires 255.27.

2-[(3-Nitrophenyl)aminocarbonyl]benzoic acid (1H). Heating was required to dissolve 3-nitroaniline in the required volume of chloroform. Mixing was carried out while the amine solution was still hot and the solution was allowed to stand for 15 h. Off-white solid (89%); mp 203–205 °C (sinters), 238–241 °C (re-melts) (lit.,⁴ 202 °C, decomposes); δ_{H} (270 MHz; (CD₃)₂SO; Me₄Si) 7.60–7.74 (m, 4H, aryl protons), 7.93–8.02 (m, 3H, aryl protons), 8.77 (t, 1H, aryl protons), 10.85 (s, 1H, CO₂H), 13.15 (br s, 1H, NH); δ_{C} (68 MHz; (CD₃)₂SO; Me₄Si) 113.09, 117.45, 124.94, 127.29, 129.17, 129.25, 129.60, 131.39, 137.71, 140.02, 147.34, 166.52, 167.33 (13 signals observed); ν_{max} /cm⁻¹ 3304 (NH), 1706 (C=O acid), 1672, 1656 (C=O amide). *M_r* Found: 287.3. C₁₄H₁₀N₂O₅ requires 286.24.

2-[(4-Nitrophenyl)aminocarbonyl]benzoic acid (1I). A solution of phthalic anhydride and a solution of 4-nitroaniline, prepared as described above, were both raised to bp. After mixing, the solution was stoppered and allowed to stand at rt for 50 h. Yellow solid (97%); mp 190 °C (sinters, decomposes), 263–264 °C (re-melts) (lit.,^{4,27} 192–193 °C, decomposes, 186 °C); δ_{H} (270 MHz; (CD₃)₂SO; Me₄Si) 7.60–7.74 (m, 3H, aryl protons), 7.96 (coincident d, 3H, aryl protons), 8.28 (d, 2H, aryl protons), 11.00 (s, 1H, CO₂H), 13.21 (br s, 1H, NH); δ_{C} (68 MHz; (CD₃)₂SO; Me₄Si) 118.66, 124.49, 127.31, 129.18, 129.24, 129.33, 131.51, 137.75, 141.70, 145.08, 166.44, 167.55; ν_{max} /cm⁻¹ 3313 (NH), 1714 (C=O acid), 1652 (C=O amide). *M_r* Found: 288.0. C₁₄H₁₀N₂O₅ requires 286.24.

2-(Phenylaminocarbonyl)benzoic acid (1J). White solid (94%); mp 167–168 °C (decomposes) (lit.,^{4,27} 169 °C, decomposes); δ_{H} (270 MHz; (CD₃)₂SO; Me₄Si) 7.06 (t, 1H, aryl proton), 7.32 (t, 2H, aryl protons), 7.51–7.70 (m, 5H, aryl protons), 7.87 (d, 1H, aryl proton), 10.30 (s, 1H, CO₂H), 13.00 (br s, 1H, NH); δ_{C} (68 MHz; (CD₃)₂SO; Me₄Si) 119.17, 122.92, 127.33, 128.17, 128.91, 129.10, 129.52, 131.23, 138.43, 139.05, 166.75, 166.83; ν_{max} /cm⁻¹ 3333 (NH), 1722 (C=O acid), 1653 (C=O amide). *M_r* Found: 246.3. C₁₄H₁₁NO₃ requires 241.25.

2-[(4-Sulfonatophenyl)aminocarbonyl]benzoic acid: pyridinium (monohydrate) (1K). Phthalic anhydride (3.70 g) and sulfanilic acid (4.33 g) were added to DMF (100 cm³). After the addition of pyridine (2.0 cm³), the mixture was heated with stirring to 100 °C for 20 min. At this point the majority of the solid material had dissolved. The mixture was then poured into acetone (400 cm³) and cooled in an ice bath for 20 min. The crude product was filtered under vacuum, washed well with diethyl ether to remove any remaining DMF, and dried at 60 °C. White solid (8.1 g, 81%). Material was purified for analysis by recrystallisation from water (about 5 cm³ g⁻¹) and was isolated as a monohydrate; mp 168–169 °C (decomposes); δ_{H} (270 MHz; (CD₃)₂SO; Me₄Si) 6.0–13.00 approx. (2H, NH; 2H, H₂O), 7.55–7.69 (m, 7H, aryl protons), 7.89 (d, 1H, aryl proton), 8.10 (t, 2H, aryl protons), 8.63 (t, 1H, aryl proton), 8.96 (d, 2H, aryl protons), 10.46 (s, 1H, CO₂H); δ_{C} (68 MHz; (CD₃)₂SO; Me₄Si) 118.08, 125.61, 126.81, 127.32, 129.00, 129.07, 129.41, 131.28, 138.21, 139.29, 141.58, 142.26, 145.82, 166.73, 166.80; ν_{max} /cm⁻¹ 3551, 3451 (NH), 1708 (C=O acid), 1670 (C=O amide). Found: C, 54.46; H, 4.31; N, 6.59. C₁₉H₁₈N₂O₆S (monohydrate) requires C, 54.54; H, 4.34; N, 6.70%. *M_r* Found: 401.7. C₁₉H₁₆N₂O₆S (anhydrous solid) requires 400.41.

Substituted phthalimides

The substituted phthalimides were prepared by the following general method, unless specified otherwise.

The appropriate substituted phthalanilic acid (**1A–1K**, 1.0 g) was added to glacial acetic acid (10 cm³) and heated in a water

bath at 80 °C for 2 h. The solution was then cooled to rt and left for 1 h. The resulting precipitate was filtered under vacuum, washed well with diethyl ether, and dried at 100 °C. No further purification proved necessary, except where details are given.

2-(4-Carboxyphenyl)-1H-isoindole-1,3(2H)-dione (2A). Compound **1A** (1.0 g) was added to glacial acetic acid (25 cm³) and heated under reflux for 1.5 h. The solution was cooled to rt and water (25 cm³) added. After 15–30 min the solid product was recovered by the general method above. White solid (73%); recrystallised from methanol; mp 285–286 °C; δ_{H} (270 MHz; (CD₃)₂SO; Me₄Si) 7.64 (d, 2H, aryl protons), 7.89–7.99 (m, 4H, aryl protons), 8.12 (d, 2H, aryl protons), 10.0–16.0 approx. (1H, CO₂H); δ_{C} (68 MHz; (CD₃)₂SO; Me₄Si) 123.05, 126.43, 129.34, 129.46, 130.90, 134.27, 135.25, 165.90, 166.03; ν_{max} /cm⁻¹ 1721 (C=O imide), 1696 (C=O acid); *m/z* 267 (M⁺, 100%), 223 (51), 104 (38), 76 (62). Found: C, 67.28; H, 3.38; N, 5.17. C₁₅H₉NO₄ requires C, 67.42; H, 3.39; N, 5.24%.

2-(3-Chlorophenyl)-1H-isoindole-1,3(2H)-dione (2B). White solid (58%), recrystallised from methanol; mp 161–163 °C (lit.,¹⁸ 163 °C); δ_{H} (270 MHz; (CD₃)₂SO; Me₄Si) 7.45–7.62 (m, 4H, aryl protons), 7.88–8.00 (m, 4H, aryl protons); δ_{C} (68 MHz; (CD₃)₂SO; Me₄Si) 123.00, 125.56, 126.65, 127.46, 129.91, 130.92, 132.33, 132.73, 134.22, 165.89; ν_{max} /cm⁻¹ 1720 (C=O imide); *m/z* 259 (M⁺, 34%), 257 (M⁺, 100), 215 (14), 213 (44), 178 (23), 76 (32).

2-(4-Chlorophenyl)-1H-isoindole-1,3(2H)-dione (2C). White solid (61%); mp 194–195 °C (lit.,¹⁸ 196 °C); δ_{H} (270 MHz; (CD₃)₂SO; Me₄Si) 7.48–7.62 (m, 4H, aryl protons), 7.90–8.00 (m, 4H, aryl protons); δ_{C} (68 MHz; (CD₃)₂SO; Me₄Si) 122.92, 128.30, 128.50, 130.23, 130.93, 131.91, 134.13, 165.95; ν_{max} /cm⁻¹ 1715 (C=O imide); *m/z* 259 (M⁺, 35%), 257 (M⁺, 100), 215 (15), 213 (44), 178 (23), 76 (30).

2-(4-Hydroxyphenyl)-1H-isoindole-1,3(2H)-dione (2D). White solid (80%); mp 288 °C (sinters), 293 °C (melts) (lit.,¹⁹ 294 °C); δ_{H} (270 MHz; (CD₃)₂SO; Me₄Si) 6.88 (d, 2H, aryl protons), 7.22 (d, 2H, aryl protons), 7.86–7.97 (m, 4H, aryl protons), 9.76 (s, 1H, OH); δ_{C} (68 MHz; (CD₃)₂SO; Me₄Si) 114.91, 122.30, 122.75, 128.23, 131.00, 133.98, 156.51, 166.57; ν_{max} /cm⁻¹ 3407 (OH), 1715 (C=O imide); *m/z* 239 (M⁺), 195, 104, 76.

2-(3-Methoxyphenyl)-1H-isoindole-1,3(2H)-dione (2E). Off-white solid (30%); recrystallised from methanol; mp 125–126 °C (lit.,¹⁴ 128 °C); δ_{H} (270 MHz; (CD₃)₂SO; Me₄Si) 3.79 (s, 3H, OCH₃), 7.02–7.07 (m, 3H, aryl protons), 7.45 (t, 1H, aryl proton), 7.88–7.98 (m, 4H, aryl protons); δ_{C} (68 MHz; (CD₃)₂SO; Me₄Si) 55.24, 112.96, 113.20, 119.14, 122.89, 129.05, 130.93, 132.39, 134.11, 158.72, 166.15; ν_{max} /cm⁻¹ 1725 (C=O imide); *m/z* 253 (M⁺, 100%), 76 (16).

2-(4-Methoxyphenyl)-1H-isoindole-1,3(2H)-dione (2F). Bright yellow solid (78%). Recrystallised from methanol; mp 159–161 °C (lit.,^{17,18} 162, 159 °C); δ_{H} (270 MHz; CD₃CO₂D; Me₂Si(CD₂)₂CO₂Na) 3.84 (s, 3H, OCH₃), 7.04 (d, 2H, aryl protons), 7.36 (d, 2H, aryl protons), 7.80–7.86 (m, 2H, aryl protons), 7.91–7.97 (m, 2H, aryl protons); δ_{C} (68 MHz; CD₃CO₂D; Me₂Si(CD₂)₂CO₂Na) 55.56, 114.45, 123.81, 124.86, 128.55, 132.16, 134.63, 159.49, 168.03; ν_{max} /cm⁻¹ 1723 (C=O imide); *m/z* 253 (M⁺, 100%), 238 (48), 210 (11), 76 (15).

2-(4-Methylphenyl)-1H-isoindole-1,3(2H)-dione (2G). White solid (73%); mp 203–204 °C (lit.,^{17,18} 204, 209 °C); δ_{H} (270 MHz; (CD₃)₂SO; Me₄Si) 2.37 (s, 3H, CH₃), 7.30 (s, 4H, aryl protons), 7.87–7.97 (m, 4H, aryl protons); δ_{C} (68 MHz; (CD₃)₂SO; Me₄Si) 20.82, 122.79, 126.62, 128.68, 128.73, 130.95, 134.02, 136.96, 166.27; ν_{max} /cm⁻¹ 1723 (C=O imide); *m/z* 237 (M⁺, 100%), 193 (41), 104 (13), 76 (24).

2-(3-Nitrophenyl)-1H-isoindole-1,3(2H)-dione (2H). Compound **1H** (1.0 g) was added to glacial acetic acid (25 cm³) and heated under reflux for 1.5 h. The solution was cooled to rt and water (25 cm³) added. After 15–30 min the solid product was recovered by the general method above. Off-white solid (78%); mp 242–243 °C (lit.,¹⁷ 244–246 °C); δ_{H} (270 MHz; (CD₃)₂SO; Me₄Si) 7.85 (t, 1H, aryl proton), 7.91–8.05 (m, 5H, aryl protons), 8.28–8.34 (m, 1H, aryl proton), 8.42 (t, 1H, aryl proton); δ_{C} (68 MHz; (CD₃)₂SO; Me₄Si) 121.51, 122.17, 123.10, 129.74, 130.96, 132.46, 133.16, 134.31, 147.16, 165.80; ν_{max} /cm⁻¹ 1727 (C=O imide); *m/z* 268 (M⁺, 100%), 222 (43), 104 (29), 76 (31).

2-(4-Nitrophenyl)-1H-isoindole-1,3(2H)-dione (2I). Compound **1I** (1.0 g) was added to glacial acetic acid (25 cm³) and heated under reflux for 1.5 h. The solution was cooled to rt and water (25 cm³) added. After 15–30 min the solid product was recovered by the general method above. Yellow solid (69%); mp 266–267 °C (lit.,^{17,18,29} 267–268, 274, 271–272 °C); δ_{H} (270 MHz; (CD₃)₂SO; Me₄Si) 7.77–7.84 (m, 2H, aryl protons), 7.92–8.05 (m, 4H, aryl protons), 8.38–8.45 (m, 2H, aryl protons); δ_{C} (68 MHz; (CD₃)₂SO; Me₄Si) 123.16, 123.64, 127.16, 130.89, 134.39, 137.19, 145.49, 165.60; ν_{max} /cm⁻¹ 1733 (C=O imide); *m/z* 268 (M⁺, 100%), 238 (35), 104 (34), 76 (46).

2-Phenyl-1H-isoindole-1,3(2H)-dione (2J). White solid (75%); mp 206–207 °C (lit.,^{17–19,30} 205, 217, 211, 210 °C); δ_{H} (270 MHz; (CD₃)₂SO; Me₄Si) 7.41–7.58 (m, 5H, aryl protons), 7.88–8.01 (m, 4H, aryl protons); δ_{C} (68 MHz; (CD₃)₂SO; Me₄Si) 122.89, 126.85, 127.50, 128.27, 130.97, 131.33, 134.1, 166.20; ν_{max} /cm⁻¹ 1702 (C=O imide); *m/z* 223 (M⁺, 100%), 179 (73), 104 (15), 76 (33).

2-(4-Sulfonatophenyl)-1H-isoindole-1,3(2H)-dione: pyridinium (2K). Compound **1K** (1.0 g) was refluxed in glacial acetic acid (20 cm³) for 1.5 h. After cooling the solution was filtered to remove traces of insoluble solid. Diethyl ether (50 cm³) was added and the resulting precipitate filtered, washed well with diethyl ether and dried at 100 °C. Off-white solid (63%); mp 222–223 °C; δ_{H} (270 MHz; (CD₃)₂SO; Me₄Si) 4.0–8.0 approx. (1H, NH), 7.44 (d, 2H, aryl protons), 7.79 (d, 2H, aryl proton), 7.90–8.00 (m, 4H, aryl protons), 8.10 (t, 2H, aryl protons), 8.64 (t, 1H, aryl proton), 8.97 (d, 2H, aryl protons); δ_{C} (68 MHz; (CD₃)₂SO; Me₄Si) 122.94, 125.56, 126.21, 126.70, 130.93, 131.39, 134.18, 141.59, 145.65, 147.02, 166.17; ν_{max} /cm⁻¹ 1712 (C=O imide). Found: C, 58.95; H, 3.67; N, 7.22. C₁₉H₁₄N₂O₅S requires C, 59.68; H, 3.69; N, 7.33%.

3-[(4-Methoxyphenyl)imino]-1(3H)-isobenzofuran-1-one (4F)

Compound **1F** (2.0 g) was suspended by magnetic stirring in dry 1,4-dioxane (20 cm³) and treated with TFAA (1.7 cm³). After stirring for 30 min the mixture was poured into cold water, the solid product was collected, washed with 10% NaHCO₃ solution, then water and finally recrystallised from aqueous acetone. Yellow solid (65%); mp 134–136 °C (lit.,²² 134 °C); δ_{H} (270 MHz; (CD₃)₂SO; Me₄Si) 3.79 (s, 3H, OCH₃), 7.02 (d, 2H, aryl protons), 7.42 (d, 2H, aryl protons), 7.84–8.12 (m, 4H, aryl protons); δ_{C} (68 MHz; (CD₃)₂SO; Me₄Si) 55.22, 113.8, 122.6, 124.68, 125.76, 126.72, 132.78, 135.23, 136.01, 145.44, 157.01, 164.04 (12 signals observed); ν_{max} /cm⁻¹ 1798 (C=O), 1692 (C=N).

Kinetic studies

Kinetic studies were carried out using a single beam diode array UV spectrophotometer with a circulating water cell heater. Solutions of **1A–1K** were prepared in absolute ethanol to an appropriate concentration, so that when 1–2 drops were added to the reaction solvent in a 1 cm, stoppered quartz cell, an absorbance of 0.5 to 1.5 was obtained at 275 nm. As soon as

possible after mixing, changes in absorbance were monitored. In all cases runs were made at least in duplicate and the average values are reported. Agreement between observed rate constants for consecutive runs was good ($\pm 5\%$), and on different days with different batches of solvents and reactants the reproducibility was never worse than $\pm 15\%$.

Molar absorptivity measurements were made by determination of the gradients of plots of absorbance against concentration for each substance. A fixed volume (3.0 cm^3) of solvent was added to the cuvette, to which aliquots (usually $1 \times 10^{-5} \text{ dm}^3$) of stock solutions were added before each absorbance reading was taken.

Acknowledgements

Sincere thanks are due to Kath Shelley and Dave Townrow for their assistance with NMR spectra and to Keith Holding for help with GC-MS analysis.

References

- 1 R. Shimazawa, H. Takayama, Y. Fujimoto, M. Komoda, K. Dodo, R. Yamasaki, R. Shirai, Y. Koiso, K. Miyata, F. Kato, M. Kato, H. Miyachi and Y. Hashimoto, *J. Enzyme Inhib.*, 1999, **14**, 259.
- 2 V. Bailleux, L. Vallee, J. P. Nuyts and J. Vamecq, *Chem. Pharm. Bull.*, 1994, **42**, 1817.
- 3 Y. Shibata, K. Sasaki, Y. Hashimoto and S. Iwasaki, *Chem. Pharm. Bull.*, 1996, **44**, 156.
- 4 M. D. Hawkins, *J. Chem. Soc., Perkin Trans. 2*, 1976, 642.
- 5 M. L. Bender, Y.-L. Chow and F. J. Chloupek, *J. Am. Chem. Soc.*, 1958, **80**, 5380.
- 6 J. Brown, S. C. K. Su and J. A. Shafer, *J. Am. Chem. Soc.*, 1966, **88**, 4468.
- 7 C. J. Perry, *J. Chem. Soc., Perkin Trans. 2*, 1997, 977.
- 8 E. Hoffmann and H. Schiff-Schenav, *J. Org. Chem.*, 1962, **27**, 4686.
- 9 J. Bishop Tingle and H. F. Rolker, *J. Am. Chem. Soc.*, 1908, **30**, 1882.
- 10 G. Drefahl, F. Fischer and W. Fischer, *Ann.*, 1957, **610**, 166 (See also *Chem. Abstr.*, 1958, **52**, 9024a).
- 11 A. A. Harfoush, *Proc. Pak. Acad. Sci.*, 1977, **14**, 25 (published 1979).
- 12 W. I. Awad, A. S. Wasfi and M. J. S. Ewad, *J. Iraqi Chem. Soc.*, 1977, **2**, 5–16.
- 13 J. Demnitz, B. d. A. Monteiro, M. N. Ramos and M. R. Srivastava, *Heterocycl. Commun.*, 1997, **3**, 115.
- 14 A. Arcoria and G. Scarlata, *Ann. Chim. (Rome)*, 1964, **54**, 128.
- 15 J. W. Verbicky, Jr. and L. J. Williams, *J. Org. Chem.*, 1981, **46**, 175.
- 16 J. W. Verbicky, Jr., L. J. Williams, B. A. Dellacoletta and W. V. Ligon, Jr., *J. Org. Chem.*, 1981, **46**, 175.
- 17 R. G. R. Bacon and A. Karim, *J. Chem. Soc., Perkin Trans. 1*, 1973, 272.
- 18 M. Michman, S. Patai and Y. Wiesel, *J. Chem. Soc., Perkin Trans. 1*, 1977, 1705.
- 19 M. L. Sherrill, F. L. Schaeffer and E. P. Shoyer, *J. Am. Chem. Soc.*, 1928, **50**, 474.
- 20 P. R. Young, *J. Heterocycl. Chem.*, 1972, **9**, 371.
- 21 A. J. Kirby and P. W. Lancaster, *J. Chem. Soc., Perkin Trans. 2*, 1972, 1206.
- 22 W. R. Roderick and P. L. Bhatia, *J. Org. Chem.*, 1963, **28**, 2018.
- 23 (a) J. H. Espenson, *Chemical Kinetics and Reaction Mechanisms*, 2nd edn., McGraw-Hill, Inc., Singapore, 1995, pp. 46–48; (b) J. H. Espenson, *Chemical Kinetics and Reaction Mechanisms*, 2nd edn., McGraw-Hill, Inc., Singapore, 1995, p. 83.
- 24 (a) N. S. Isaacs, *Physical Organic Chemistry*, 2nd edn., Longman Scientific & Technical, UK and New York, 1995, pp. 381–389; (b) N. S. Isaacs, *Physical Organic Chemistry*, 2nd edn., Longman Scientific & Technical, UK and New York, 1995, pp. 152, 153.
- 25 W. P. Jencks, *Chem. Rev.*, 1972, **72**, 705.
- 26 C. D. Johnson, *The Hammett Equation*, Cambridge University Press, Cambridge, 1973, pp. 27–31.
- 27 N. V. Subba Rao and C. V. Ratnam, *J. Sci. Ind. Res., Sect. B*, 1962, **21**, 45.
- 28 R. D. Reynolds, M. J. Zeigler and D. J. Hueck, *J. Chem. Eng. Data*, 1968, **13**, 558.
- 29 C. L. Butler, Jr. and R. J. Adams, *J. Am. Chem. Soc.*, 1925, **47**, 2610.
- 30 *CRC Handbook of Chemistry & Physics*, ed. R. C. Weast, 58th edn.; Chemical Rubber Publishing Company, Florida, USA, 1977–1978, C437.